Available online at www.sciencedirect.com

ScienceDirect

journal homepage: www.elsevier.com/locate/he

Production of H_2 in the photocatalytic reactions of ethane on TiO_2-supported noble metals

*Gyula Halasi, Anita Tóth, Tamás Bánsági, Frigyes Solymosi**

MTA-SZTE Reaction Kinetics and Surface Chemistry Research Group, Rerrich Béla tér 1, H-6720 Szeged, Hungary

ARTICLE INFO

Article history:
Received 2 March 2016
Received in revised form
25 May 2016
Accepted 4 June 2016
Available online 19 June 2016

Keywords:
Photo-induced decomposition of ethane
Effects of CO_2
TiO_2-supported Pt metals
TPR studies on carbon deposit

ABSTRACT

The effect of illumination on the adsorption and reaction of ethane was investigated on TiO_2 and TiO_2-supported Pt metals. IR studies showed that new absorption bands developed as a result of illumination of the catalysts. The photocatalytic decomposition of ethane was very limited on pure TiO_2: the conversion was only ~4% at 300 K in 210 min. Deposition of Pt metals onto TiO_2 markedly enhanced the rate of photo-induced decomposition of C_2H_6. Highest conversion of C_2H_6, 23.5%, was measured over Pt/TiO_2 and the turnover frequency was also the highest on this catalyst. Addition of CO_2 to ethane exerted no influence on the photocatalysis of ethane. Surprisingly, the main gaseous product of the photocatalytic reaction is H_2 with a small amount of CH_4. Ethylene was not detected even in traces, indicating the complete degradation of C_2H_6 to H_2 and carbon containing deposit. Temperature programmed reduction (TPR) revealed that the carbonaceous deposit on the catalysts is very stable. On Rh/TiO_2 it reacted with H_2 to give CH_4 (Tp = 453 and 604 K), C_2H_6 and C_3H_8 (Tp = 602 K). Similar values were found on Pt/TiO_2. The promoting effect of metals was explained by a better separation of charge carriers induced by illumination and by the enhanced electronic interaction between metals and TiO_2.

Introduction

The conversion of alkanes into more important compounds is an important subject of heterogeneous catalysis [1–3]. There is a great variety in the reactivity of alkanes. Whereas both the decomposition and dry reforming of CH_4 requires high temperature even on the most active Rh [4,5], the reactions of C_2H_6 [6–8] and C_3H_8 [9,10] proceeds at significantly lower temperatures. This difference in the reactivity appeared in their aromatization on Mo_2C/ZSM-5. Methane was converted into benzene around 973 K [11–13], while the aromatization of C_2H_6 proceeds on the same catalyst at 873 K [14] and that of C_3H_8 at 773 K [15,16]. An alternative but less exploited way of hydrocarbons is to use them as a source of hydrogen. The production of hydrogen became a very important subject for heterogeneous catalysis. Due to the high stability of these compounds, however, their catalytic decomposition needs high temperature and very effective catalysts [17–20]. Catalytic cracking of C_6–C_7 paraffins on HZSM-5 proceeds at somewhat lower temperatures, but it yields several H-containing compounds beside H_2 [21–26]. As in several other cases one expects that the activation of C–H bond in lower alkanes on solid surfaces can be achieved by illumination. In the present work we examine the effect of photocatalysis on the decomposition of C_2H_6 and its reaction with CO_2 on TiO_2-

* *Corresponding author*. Fax: +36 62 544 106.
E-mail address: fsolym@chem.u-szeged.hu (F. Solymosi).
http://dx.doi.org/10.1016/j.ijhydene.2016.06.020

supported Pt metals. Surprisingly, relatively few works have been devoted to the photocatalytic reactions of hydrocarbons, most of the studies dealt with the photo-oxidation of light alkanes [27–34].

Experimental

Methods

Photocatalytic reaction was followed in the same way as described in our previous papers [35], equipped with a 500 W medium pressure mercury vapor lamp (TQ 718, Heraeus Noble light, Germany) as a light source. In some experiments we applied a 15 W germicide lamp, which emits predominantly in the wavelength of 250–440 nm, and its maximum intensity is at 254 nm. For the visible photocatalytic experiments another type of lamp was used (Lighttech GCL 307T5L/GOLD) with 400–640 nm wavelength range and two maximum intensities at 453 and 545 nm. Note that this lamp also emits below 400 nm. The approximate light intensity at the catalyst films is 59.4 mW/cm^2 for the 500 W lamp, 3.9 mW/cm^2 for the germicide lamp and 2.1 mW/cm^2 for the lamp used for experiments in the visible light. The photoreactor (volume: 670 ml) consists of two concentric quartz glass tubes fitted one into the other and a centrally positioned lamp. It is connected to a gas-mixing unit serving for the adjustment of the composition of the gas or vapor mixtures to be photolyzed in situ. The carrier gas was Ar, which was mixed with C_2H_6 (~1.5%, 330 μmol). In the study of the effects of CO_2, its amount was varied between ~1.5–4.5%. The gas-mixture was circulated by a diaphragm pump. The reaction products were analyzed with an Agilent 4890 gas chromatograph equipped with PORAPAK 1/2Q + PORAPAK 1/2S packed and Equity-1 capillary column. The sampling loop of the GC was 500 μl. The amount of all products was related to this loop. The conversion of C_2H_6 was calculated taking into account the amount of C_2H_6 consumed. This value agreed well with that one based on the H basis, e.g. taking into account the H content of the C_2H_6 and the amount of H_2 formed.

For FTIR studies a mobile IR cell housed in a metal chamber was used [35]. Infrared spectra were recorded with a Biorad (Digilab. Div. FTS 155) instrument. Samples were illuminated by the full arc of a Hg lamp (100 W LPS-220, PTI) outside the IR sample compartment. The filtered light passed through a high-purity CaF_2 window into the cell. All the spectra presented in this study are difference spectra.

In the temperature programmed desorption (TPD) the heating rate was 5 K/ml and the flow of Ar was 20 ml/min. The temperature programmed reduction (TPR) was carried out in H_2 flow (15 ml/min) with a ramp of 5 K/min heating rate from about 300 K up to 1173 K. Desorption products were analysed by gas chromatography. For TPR experiments 7 previously used catalysts samples (30 × 10 mm) were applied.

Diffuse reflectance spectra of TiO_2 samples were obtained using an UV/Vis spectrophotometer (OCEAN OPTICS, Typ.USB 2000) equipped with a diffuse reflectance accessory. The surface area of the catalysts was determined by BET method with N_2 adsorption at ~100 K. The dispersion of metals was determined by the adsorption of H_2 at room temperature.

Materials

TiO_2 (Hombikat, UV 100; pure anatase, 300 m^2/g) and Al_2O_3 (Degussa C, 100 m^2/g), CeO_2 (Alfa Aesar, 50 m^2/g) and ZnO (Strem Chem, 40 m^2/g) were used as a supports for Pt metals. The following salts of Pt metals were used: $Pd(NO_3)_2$, H_2IrCl_6, $RhCl_3 \cdot 3H_2O$, $H_2PtCl_6 \cdot 6H_2O$ and $RuCl_3 \cdot 3H_2O$. All supported Pt metal catalysts were prepared by a deposition-precipitation method.

For the preparation of N-doped samples TiO_2 was reacted with NH_3 [36]. Titanium tetrachloride was used as titanium precursor. The $TiCl_4$ was carefully added into 150 ml Milli-Q water with gentle stirring in ice-water bath. After then the solution was heated to 323 K and 4.5 ml glacial acetic acid and 35 wt% ammonia was added dropwise with vigorous stirring until pH 8. After this step the solution was cooled down to 298 K and aging for a few days. The prepared sample was filtered and washed until pH 7 and then vacuum dried at 353 K for 12 h, followed by calcination at 723 K in flowing air for 3 h. The N–TiO_2 microtube sample is noted with "SX". The surface area of TiO_2 prepared in this way is 265 m^2/g and that of N-doped oxide is 79 m^2/g. The nitrogen content of this sample is 2.9%. The bandgaps of these TiO_2 samples have been evaluated in our previous work [37]. The bandgap energy was determined from the plots of Kubelka-Munk function $F(R_\infty)$ *vs.* wavelength. We obtained 3.02 eV for pure TiO_2 and 1.98 eV for N-doped TiO_2 microtubes. Metal-promoted TiO_2 samples were prepared by impregnating pure or doped TiO_2 with the solution of metal compounds to yield a nominal 2 wt% metal [37]. For IR studies the samples were pressed in self-supporting wafers (30 × 10 mm ~10 mg/cm^2). For photocatalytic measurements the sample (~180 mg) was sprayed onto the outer side of the inner tube from aqueous suspension. The surface of the catalyst film was 439 cm^2. The catalysts were oxidized and reduced at 573 K in the IR cell or in the catalytic reactor for 1 h. Ethane was the product of Messer with purity of 99.95% and the CO_2 was purchased from Messer, purity 99.995%.

Results

IR spectroscopic studies

To identify the surface species formed during the photocatalysis of C_2H_6 detailed IR spectroscopic studies were performed. In the case of pure TiO_2 admission of C_2H_6 into the cell gave intense absorption bands in the CH_x region at 3006, 2971, 2954, 2933, 2894 and 2831 cm^{-1}, which remained practically unaltered following the illumination. In the low frequency region, the bands at 1622 and 1445 cm^{-1}, present before illumination, clearly intensified and several new weak bands developed already after 30 min of photocatalysis. In the CH_x frequency range we obtained the same picture for TiO_2-supported metals. In the low frequency range of the IR spectra of Rh/TiO_2 the absorption band at 1618 cm^{-1} became very large after extended illumination and weak absorptions at 1442, 1382 and 1343 cm^{-1} developed. In the case of Pt/TiO_2 illumination caused only slight effect on the IR spectra of ethane. In contrast, strong bands developed at 1662, 1565, 1444, 1346 and

1220 cm^{-1} following the irradiation of C_2H_6 on Pd/TiO_2. Some IR spectra are presented in Fig. 1.

TPD measurements

The interaction of some catalysts with ethane was also examined by means of TPD measurements. The catalyst was kept in the ethane flow for 10 min at 330–350 K, then it was washed with pure Ar until it contained ethane (~20 min). Results for TiO_2 and Rh/TiO_2 support are displayed in Fig. 2. It shows that a small amount of C_2H_6 remained adsorbed on both samples, which was released with Tp = 328 K. A larger amount of CH_4 also desorbed at higher temperatures from TiO_2 with Tp = 528 and 678 K and from Rh/TiO_2 with Tp = 553 K.

Photocatalytic studies

Deposition of Pt metals on TiO_2 exerted a remarkable photocatalytic effect on the decomposition of ethane. Results are displayed in Fig. 3. Highest activity was measured on Pt/TiO_2 and Rh/TiO_2 and the lowest one on Ru/TiO_2. The main gaseous product was H_2, the amount of which increased with the length of irradiation. A small amount of CH_4 was also produced on the active catalysts (3–8%). Surprisingly, however, the formation of C_2H_4, the product of the dehydrogenation of C_2H_6 was completely missing. Calculation of the conversion on the consumption of ethane showed a good agreement with the values based on the H content of the product. However, we obtained much less values based on the carbon content of the ethane reacted and methane found.

In the case of the active Rh catalyst we examined the effect of other oxidic supports, like ZnO, CeO_2 and Al_2O_3. As shown in Fig. 4 these samples exhibited very low photoactivity. Similarly to the case of TiO_2-supported metals, the major product was H_2 with a small amount of CH_4. We also determined the photocatalytic efficiency of the oxides alone. Highest conversion, ~4%, was measured on pure TiO_2.

Detailed measurements were performed concerning the effect of CO_2. Adding CO_2 to C_2H_6 (mole ratio 1:1) exerted no influence on the photoreaction of ethane on TiO_2-supported metals. We obtained the same result when the amount of CO_2 was significantly increased ($CO_2/C_2H_6 = 3$). In harmony with this finding CO was not detected in the products. We made an extensive search for the identification of O-containing compounds. When the CO_2/C_2H_6 ratio was 3 the formation of ethanol (~0.24%) and methanol (~0.35%) was found. Interestingly the amount of CH_4 remained almost unaltered. As we are using a very powerful, 500 W medium pressure lamp, we cannot exclude the possibility that the transiently formed O-containing CH compounds underwent rapid decomposition before its identification [37].

TPR measurements

The results presented in Fig. 3 clearly indicated that illumination of C_2H_6 on TiO_2-based noble metals leads to a complete degradation of ethane to hydrogen and some kind of

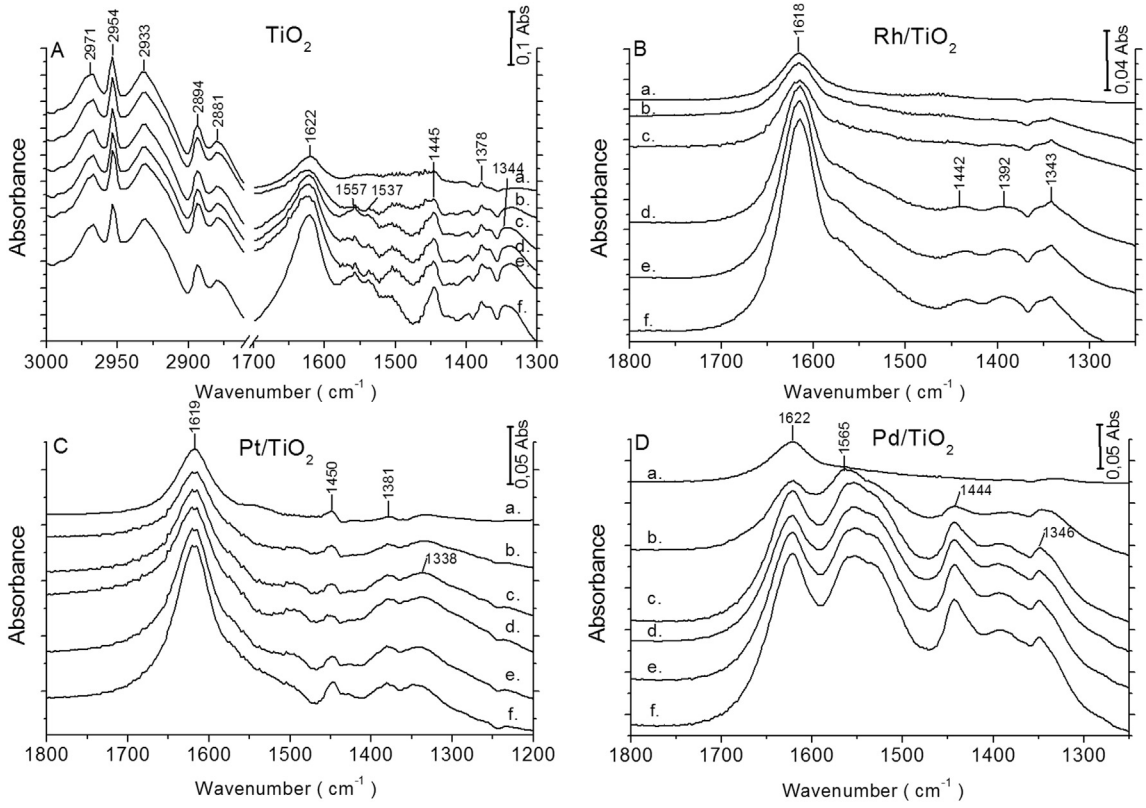

Fig. 1 – Effect of illumination on the infrared spectra of C_2H_6 on Rh/TiO_2, Pt/TiO_2, Ir/TiO_2 and TiO_2 at 300 K in time. (a) 0 min; (b) 5 min; (c) 30 min; (d) 60 min; (e) 90 min; (f) 120 min.

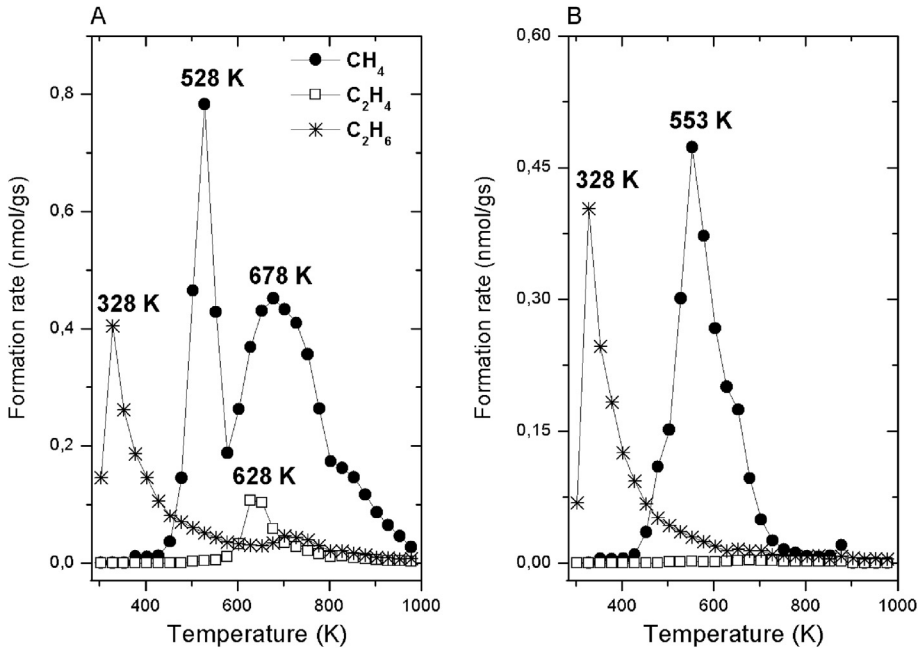

Fig. 2 – Temperature programmed desorption of C_2H_6 following its adsorption over TiO_2 (A), and Rh/TiO_2 (B) at 300 K.

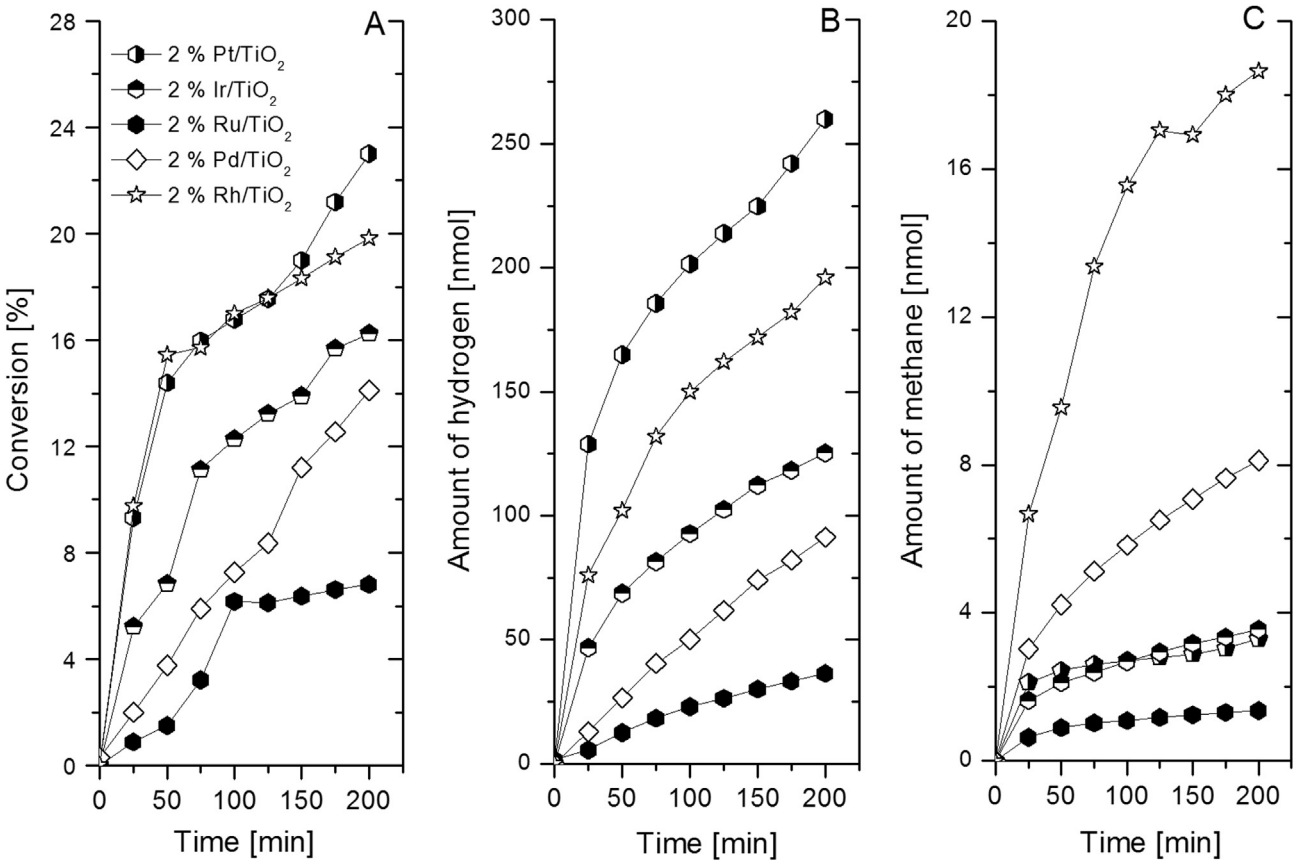

Fig. 3 – Photocatalytic reaction of C_2H_6 on various TiO_2 supported catalysts (A). Formation of H_2 (B) and CH_4 (C).

carbonaceous compound. In order to know more about this deposit the catalyst film has been removed from the photoreactor after the completion of the photocatalytic reaction, and TPR measurements were carried out in a separate reactor. Some TPR spectra are presented in Fig. 5. On Rh/TiO_2 a small amount of CH_4 was produced with a $T_p = 453$ K, and a much larger one with $T_p = 604$ K. Little amounts of ethane and propane with $T_p = 602$ K were also formed. In the case of Pt/

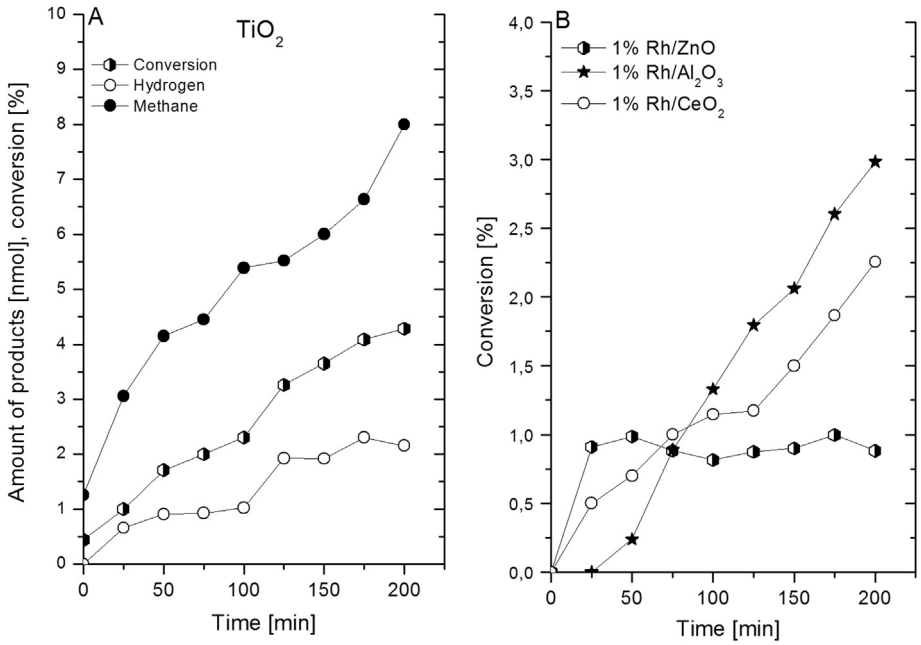

Fig. 4 – Photocatalytic reaction of C_2H_6 on TiO_2 (A) and on Rh deposited on various oxides (B).

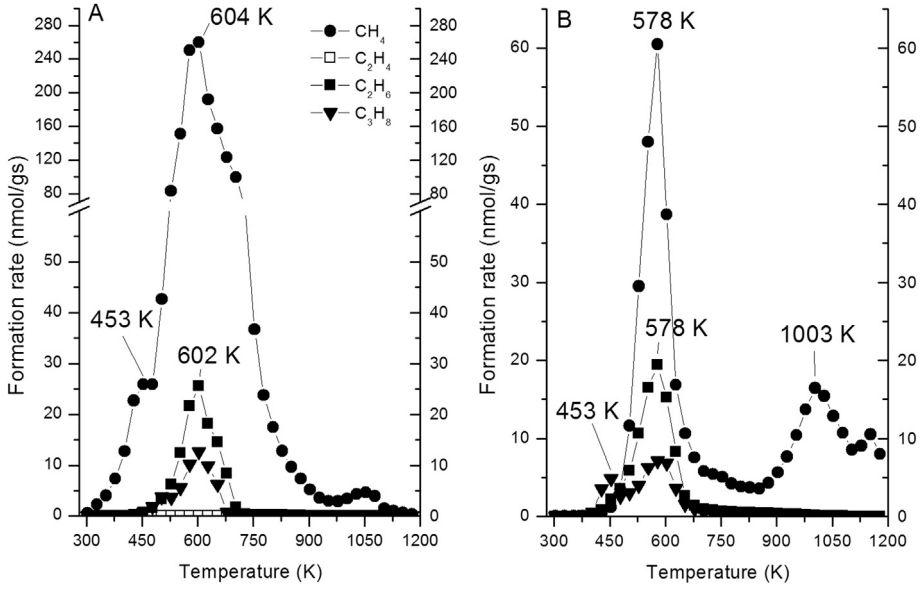

Fig. 5 – Temperature programmed reduction (TPR) following the photocatalytic reaction of C_2H_6 over Rh/TiO_2 (A) and Pt/TiO_2 (B).

TiO_2 the generation of CH_4 occurred with T_p values of 578 and 1003 K. A very tiny peak was also detected at T_p 1055 K.

Photocatalytic studies in visible light

An attempt was made to investigate the photocatalysis of C_2H_6 on Pt/TiO_2 in visible light. Unfortunately, the lamp available for such a study was less effective (15 W), so we obtained only very limited photoreaction (conversion ~0.1%). Somewhat higher photoactivity (conversion 0.2–0.3%) was measured over Pt deposited on N-doped TiO_2.

Discussion

Interaction of ethane with M/TiO_2

IR and TPD measurements indicate that ethane adsorbed both on TiO_2 and metal-containing TiO_2 at ~300 K. The amount of adsorbed ethane is only slightly larger on M/TiO_2 samples compared to pure TiO_2. Its desorption occurred at relatively low temperature from both pure and metal-containing TiO_2 (Fig. 2). The adsorption and the bonding of ethane on TiO_2 are

only slightly influenced by the presence of a small amount of metal. IR spectroscopic studies also confirmed the existence of molecularly bonded ethane at ~300 K. As a result of illumination, however, the absorption peaks developed at ~1618, ~1450, ~1442, ~1343 and ~1392 cm^{-1}, which can be attributed to the different vibration of adsorbed $CH_2{=}CH_2$ formed (see Table 1).

Catalytic study

Pure TiO_2 exhibited only a very modest photocatalytic activity for the reaction of C_2H_6: the conversion was only ~4% in 210 min. Deposition of Pt metals on TiO_2, however, markedly enhanced its effect. On the basis of conversion measured in 210 min we obtained the following activity order for TiO_2-supported metals: Pt/TiO_2 (23%), Rh/TiO_2 (20%), Ir/TiO_2 (16%), Pd/TiO_2 (14%), Ru/TiO_2 (7%). Comparison on the basis of turnover over frequency gave very similar order (Table 2).

The possible reason of the low photoactivity of TiO_2 is that the recombination of the charges induced by illumination

$$TiO_2 + h\nu = h^+ + e^- \quad (1)$$

$$h^+ + e^- = h\nu \quad (2)$$

is very fast on TiO_2. The deposition of Pt metals onto TiO_2, however, markedly enhanced the extent of photo-effect of TiO_2. This promoting effect of metals in photocatalytic processes is generally explained by the better separation of the charge carriers generated in the primary process [38,39], which provides a greater possibility for the activation of C_2H_6

$$C_2H_6 + e^- = C_2H_6^{\delta-} \quad (3)$$

$$C_2H_6^{\delta-} = C_2H_{5(a)} + H_{(a)} + e^- \quad (4)$$

It can be also assumed that the Schottky barrier at metal/TiO_2 interface can function as efficient barrier preventing electron–hole recombination [40,41]. In the case of Au catalyst Wu et al. [42] pointed out that smaller metal particles induce more negative Fermi level shift than the larger particles. In addition the surface plasmon resonance absorption may also contribute to the total absorption thereby to the enhanced photoactivity of Au/TiO_2 catalyst [43–45]. As the work function of Pt metals are higher (4.71–5.16 eV) than that of TiO_2 (4.6 eV), we can also expect the transfer of electrons from TiO_2 to Pt metals at the M/TiO_2 interface contributing also to the enhanced activation of adsorbed molecules. The role of the electron transfer in the enhanced catalytic effect of TiO_2 supported metals catalysts has been assumed and confirmed long time ago [46,47] and this idea has been generally used since then.

As regards the further steps we could assume the decomposition of C_2H_5 radical to C_2H_4

$$C_2H_{5(a)} = C_2H_{4(g)} + H_{(a)} \quad (5)$$

or as was found on many metal surfaces [48,49], its recombination

$$C_2H_{5(a)} = C_4H_{10(a)} \quad (6)$$

The fact that neither C_2H_4 nor C_4H_{10} was detectable in the products suggests that the lifetime of transiently formed C_2H_5 or C_xH_y is very short, and instead of their coupling reactions they underwent fast photo-generated degradation resulting in some kind of carbonaceous deposit onto the catalyst.

$$C_2H_{5(a)} = C_{(s)} + 2.5\ H_2 \quad (7)$$

As TPR measurements revealed it reacts with H_2 around 600 K.

A surprising result is that adding CO_2 to C_2H_6 exerted no influence on the photo-induced reaction of C_2H_6. Several previous studies showed that illumination activates the CO_2 molecule leading to the formation of negatively charged CO_2^-, which is much more reactive than the neutral CO_2 [50,51]. The

Table 1 – Vibrational frequencies following C_2H_6 adsorption, and illumination and their assignments.

Assignment	C_2H_6 gas [6]	C_2H_6/ZSM-5 [6],[b]	C_2H_6/TiO_2 [present study]	$C_2H_6/Rh/TiO_2$ [present study]	$C_2H_6/Pt/TiO_2$ [present study]	$C_2H_6/Pd/TiO_2$ [present study]
$\nu_a(CH_3)$	2985	2969	2971	2983	2964	2965
$\nu_a(CH_3)$	2969[a]	2940	2954	2952	2952	2952
$\nu_s(CH_3)$	2954[a]	2918	2933			
$\nu_s(CH_3)$	2896	2881	2894	2889	2890	2890
$2\delta_a(CH_3)$			[c]1622 (I)	[c]1618 (I)	[c]1619 (I)	1622 (I)
$\delta_a(CH_3)$	1469	1445			[c]1450	
$\delta_a(CH_3)$	1468[a]	–	[c]1445 (II)	[c]1442 (II)		[c]1444 (II)
$\delta_s(CH_3)$	1338[a]	–	[c]1344 (III)	[c]1343 (III)	[c]1338 (III)	[c]1346 (III)
$\delta_s(CH_3)$	1379	1371	[c]1378	[c]1392	[c]1381	[c]1395
$\rho(CH_3)$	1190[a]					

I. ν_{as} of $CH_2{=}CH_2$.
II. δ_a of $CH_2{=}CH_2$.
III. δ_s of $CH_2{=}CH_2$.
[a] Not IR active.
[b] Temperature, 146–186 K.
[c] Developed as a result of illumination.

Table 2 – Some characteristic data for the catalysts and catalytic reaction on M/TiO_2.

Samples	Dispersion of the metals (in %)	Work function of metals (in eV)	Conversion of C_2H_6 in 210 min (in %)	Turnover frequency in 200 min (TOF_{H_2}) (1/s)
Pt/TiO_2	13.0	5.70	23.5	0.312
Rh/TiO_2	16.0	4.68	20.0	0.081
Ir/TiO_2	54.0	5.76	16.3	0.031
Pd/TiO_2	26.0	5.12	14.0	0.011
Ru/TiO_2	6.0	4.78	7.0	0.020

TOF_{H_2}: the amount of H_2 formed in 210 min related to the number of metal atoms.
Work function of pure TiO_2 is 4.6 eV.

importance of the activation of CO_2 appeared in our recent study dealing with the catalytic and photocatalytic reaction of $H_2 + CO_2$ on Au deposited on various n-type oxides [52,53]. Depending on the nature of the supports the thermal catalytic reaction proceeds above 475–500 K leading exclusively to the formation of CO and H_2O. Methane and methanol formed only in trace quantities. Photocatalysis, however, induced the reaction giving CH_4 even at room temperature. The highest conversion on the most active Au/TiO_2 was 3–5% in 200 min. In the present case, however, there was no sign of any effect or involvement of CO_2 in the photo-induced decomposition of C_2H_6. Further investigations are clearly needed.

Conclusions

(i) A strongly adsorbed C_2H_6 decomposed on TiO_2-supported Pt metals only above 550 K yielding mainly CH_4.
(ii) Photocatalytic decomposition of C_2H_6 is very limited on TiO_2.
(iii) Deposition of noble metals on TiO_2 markedly enhances the extent of the photocatalytic reaction leading to the formation of hydrogen and carbonaceous deposit with a small amount of CH_4.
(iv) Addition of CO_2 to C_2H_6 exerted no influence of the photoreaction of C_2H_6.

Acknowledgments

This work was supported by National Research, Development and Innovation Office - NKFIH under contract number PD 115769.

REFERENCES

[1] Bibby DM, Chang CD, Howe RF, Yurchak S, editors. Methane conversion: studies on surface science and catalysis, vol. 36. Amsterdam: Elsevier; 1998.
[2] Ono Y. Transformation of lower alkanes into aromatic hydrocarbons over ZSM-5 zeolites. Catal Rev Sci Eng 1992;34:179–226.
[3] Solymosi F. Molecular chemistry of alkane activation. Aromatization of hydrocarbons on supported Mo_2C catalysts. In: Derouane EG, Parmon V, Lemos F, Ribeiro FR, editors. Sustainable strategies for the upgrading of natural gas: fundamentals, challenges and opportunities. Springer; 2005. p. 25–50.
[4] Rostrup-Nielsen JR. Syngas for C_1-chemistry. Limits of the steam reforming process. Stud Surf Sci Catal 1988;36:73–8.
[5] Rostrup-Nielsen JR, Aasberg-Petersen K, Schoubye PS. The role of catalysis in the conversion of natural gas for power generation. Stud Surf Sci Catal 1997;107:473–88.
[6] Solymosi F, Szőke A, Óvári L. Decomposition of ethane and its reaction with CO_2 over Rh/ZSM-5 catalyst. J Catal 1999;186:269–78.
[7] Solymosi F, Németh R. The oxidative dehydrogenation of ethane with CO_2 over Mo_2C/SiO_2 catalyst. Catal Lett 1999;62:197–200.
[8] Zhu H, Rosenfeld DC, Anjum DH, Sangaru SS, Saih Y, Ould-Chikh S, et al. Ni-Ta-O mixed oxide catalysts for the low temperature oxidative dehydrogenation of ethane to ethylene. J Catal 2015;329:291–306.
[9] Solymosi F, Tolmacsov P. Decomposition of propane and its reactions with CO_2 over alumina-supported Pt metals. Catal Lett 2002;83:183–6.
[10] Solymosi F, Tolmacsov P, Süli Zakar T. Dry reforming of propane over supported Re catalyst. J Catal 2005;233:51–9.
[11] Solymosi F, Erdőhelyi A, Szőke A. Dehydrogenation of methane on supported molybdenum oxides. Formation of benzene from methane. Catal Lett 1995;32:43–53.
[12] Wang D, Lunsford JH, Rosynek MP. Characterization of a Mo/ZSM-5 catalyst for the conversion of methane to benzene. J Catal 1997;169:347–58.
[13] Solymosi F, Cserényi J, Szőke A, Bánsági T, Oszkó A. Aromatization of methane over supported and unsupported Mo-based catalysts. J Catal 1997;165:150–61.
[14] Solymosi F, Szőke A. Conversion of ethane into benzene on Mo_2C/ZSM-5 catalyst. Appl Catal A Gen 1998;166:225–35.
[15] Solymosi F, Németh R, Óvári L, Egri L. Reactions of propane on supported Mo_2C catalysts. J Catal 2000;195:316–25.
[16] Yuan S, Hamid SBDA, Li Y, Ying P, Xin Q, Derouane EG, et al. Preparation of Mo_2C/HZSM-5 and its catalytic performance for the conversion of n-butane into aromatics. J Mol Catal A Chem 2002;184:257–66.
[17] Belgued M, Pareja P, Amariglio A, Amariglio H. Conversion of methane into higher hydrocarbons on platinum. Nature 1991;352:789–90.
[18] Koerts T, van Santen A. A low-temperature reaction sequence for methane conversion. J Chem Soc Chem Commun 1991:1281–3.
[19] Solymosi F, Erdőhelyi A, Cserényi J, Felvégi A. Decomposition of CH_4 over supported Pd catalysts. J Catal 1994;147:272–8.
[20] Solymosi F, Cserényi J. Decomposition of CH_4 over supported Ir catalysts. Catal Today 1994;21:561–9.
[21] Abbot J. Cracking reactions of C_6 paraffins on HZSM-5. Appl Catal 1990;57:105–25.
[22] Zhao Y, Bamwenda GR, Wojciechowski BW. Cracking selectivity patterns in the presence of chain mechanisms. The cracking of 2-methylpentane. J Catal 1993;142:465–89.
[23] Yaluris G, Rekoske JE, Aparicio RJ, Madon RJ, Dumesic JA. Isobutane cracking over Y-zeolites. I. Development of a kinetic-model. J Catal 1995;153:54–64.
[24] Krannila H, Haag WO, Gates BC. Monomolecular and biomolecular mechanisms of paraffin cracking: n-butane cracking catalyzed by HZSM-5. J Catal 1992;135:115–24.

[25] Wojciechowski BW. The reaction mechanism of catalytic cracking: quantifying activity, and catalyst decay. Catal Rev Sci Eng 1998;40:209–328.
[26] Corma A, Mengual J, Miguel PJ. Catalytic cracking of n-alkane naphtha: the impact of olefin addition and active sites differentiation. J Catal 2015;330:520–32.
[27] Zhong SH, Zhao C, Wang X, Mei CS. Photocatalysis synthesis crylic acid from carbon dioxide and ethene over Cu/ZnOTiO$_2$ catalysts. In: Proceedings of the Thirteenth International Congress on Catalysis Paris; 2004. p. 2419–21.
[28] Wang XT, Zhong SH, Xiao XF. Photo-catalysis of ethane and carbon dioxide to produce hydrocarbon oxygenates over ZnO-TiO$_2$/SiO$_2$ catalyst. J Mol Catal A Chem 2005;229:87–93.
[29] Ward MD, Brazdil JF, Mehandru SP, Anderson AB. Methane photoactivation on copper molybdate: an experimental and theoretical study. J Phys Chem 1987;91:6515–21.
[30] Djeghri N, Formenti M, Juillet F, Teichner SJ. Photointeraction on the surface of titanium dioxide between oxygen and alkanes. Faraday Discuss Chem Soc 1974;58:185–93.
[31] Hill W, Shelimov BN, Kazansky VB. Photoinduced reactions of methane with molybdena supported on silica. J Chem Soc Faraday Trans I 1987;83:2381–9.
[32] Grätzel M, Thampi KR, Kiwi J. Methane oxidation at room temperature and atmospheric pressure activated by light via polytungstate dispersed on titania. J Phys Chem 1989;93:4128–32.
[33] Wada K, Yoshida K, Takatani T, Watanabe Y. Selective photo-oxidation of light alkanes using solid metal oxide semiconductors. Appl Catal A Gen 1993;99:21–36.
[34] Brigden CT, Poulston S, Twigg MV, Walker AP, Wilkins AJJ. Photo-oxidation of short-chain hydrocarbons over titania. Appl Catal B Environ 2001;32:63–71.
[35] Halasi G, Bánsági T, Solymosi F. Photocatalytic reduction of NO with ethanol on Au/TiO$_2$. J Catal 2015;325:60–7.
[36] Xu JH, Dai WL, Li J, Cao Y, Li H, He H, et al. Simple fabrication of thermally stable apertured N-doped TiO$_2$ microtubes as a highly efficient photocatalyst under visible light irradiation. Catal Commun 2008;9:146–52.
[37] Halasi G, Ugrai I, Solymosi F. Photocatalytic decomposition of ethanol on TiO$_2$ modified by N and promoted by metals. J Catal 2011;281:309–17.
[38] Linsebigler A, Lu G, Yates Jr JT. Photocatalysis on TiO$_2$ surfaces: principles, mechanisms and selected results. Chem Rev 1995;95:735–58.
[39] Hoffmann MR, Martin ST, Choi W, Bahnemann DW. Environmental applications of semiconductor photocatalysis. Chem Rev 1995;95:69–96.
[40] Ismail AA, Bahnemann DW, Bannat I, Wark M. Gold nanoparticles on mesoporous interparticle networks of titanium dioxide nanocrystals for enhanced photonic efficiencies. J Phys Chem C 2009;113:7429–35.
[41] Alvaro M, Cojocaru B, Ismail AA, Petrea N, Ferrer B, Harraz FA, et al. Visible-light photocatalytic activity of gold nanoparticles supported on template-synthesized mesoporous titania for the decontamination of the chemical warfare agent Soman. Appl Catal B Environ 2010;99:191–7.
[42] Wu G, Chen T, Su W, Zhou G, Zong X, Lei Z, et al. H$_2$ production with ultra-low CO selectivity via photocatalytic reforming of methanol on Au/TiO$_2$ catalyst. Int J Hydrogen Energy 2008;33:1243–51.
[43] Subramanian V, Wolf EE, Kamat PV. Catalysis with TiO$_2$/gold nanocomposites. Effect of metal particle size on the Fermi level equilibration. J Am Chem Soc 2004;126:4943–50.
[44] Primo A, Corma A, Garcia H. Titania supported gold nanoparticles as photocatalyst. Phys Chem Chem Phys 2011;13:886–910.
[45] Yu K, Tian Y, Tatsuma T. Size effects of gold nanoparticles on plasmon-induced photocurrents of gold-TiO$_2$ nanocomposites. Phys Chem Chem Phys 2006;8:5417–20.
[46] Szabó ZG, Solymosi F. Influence of the defect structure of support on the activity of catalyst. In: Actes Du Deuxieme Congres International De Catalyse Paris; 1961. p. 1627–51.
[47] Solymosi F. Importance of the electric properties of supports in the carrier effect. Catal Rev 1968;1:233–55.
[48] Solymosi F. Thermal stability and reactions of CH$_2$, CH$_3$ and C$_2$H$_5$ species on the metal surfaces. Catal Today 1996;28:193–203.
[49] Zaera F. Determination of the mechanism for ethylidyne formation from chemisorbed ethylene on transition metal surfaces. J Am Chem Soc 1989;111:4240–4.
[50] Freund HJ, Messmer RP. On the bonding and reactivity of CO$_2$ on metal-surfaces. Surf Sci 1986;172:1–30.
[51] Solymosi F. The bonding, structure and reactions of CO$_2$ adsorbed on clean and promoted metal surfaces. J Mol Catal 1991;65:337–58.
[52] Farkas AP, Solymosi F. Photolysis of the CO$_2$ + K/Au(111) system. J Phys Chem C 2010;114:16979–82.
[53] Halasi G, Gazsi A, Bánsági T, Solymosi F. Catalytic and photocatalytic reactions of H$_2$ + CO$_2$ on supported Au catalysts. Appl Catal A Gen 2015;506:85–90.